

# Optimal Illumination and Color Consistency for Optical Remote-Sensing Image Mosaicking

Jiayuan Li, Qingwu Hu, and Mingyao Ai

**Abstract**—Illumination and color consistency are very important for optical remote-sensing image mosaicking. In this letter, we propose a simple but effective technique that simultaneously performs image illumination and color correction for multiview images. In this framework, we first present an uneven illumination removal algorithm based on bright channel prior, which guarantees the illumination consistency inside a single image. We then adapt a pairwise color-correction method to coarsely align the color tone between source and reference images. In this stage, we give a new single-image quality metric which combines brightness deviation, color cast, and entropy together for automatic reference-image selection. Finally, we perform a least-squares adjustment (LSA) procedure to obtain optimal illumination and color consistency among multiview images. In detail, we first perform a pairwise image matching by using SIFT algorithm; once sparse local patch correspondences obtained, the illumination and color relationship between images can be established based on a global gamma correction model; the illumination and color errors can then be minimized by LSA. Extensive experiments on both challenging synthetic and real optical remote-sensing image data sets show that it significantly outperforms the compared state-of-the-art approaches. All the source code and data sets used in this letter are made public.<sup>1</sup>

**Index Terms**—Bright channel prior (BCP), color correction, single-image quality (SIQ) metric, uneven illumination removal.

## I. INTRODUCTION

IMAGE mosaicking, which is a technique to seamlessly fuse multiple images with overlapping areas into a single composite image, has many applications in remote sensing, such as digital orthophoto map production. The quality of a mosaicked image is usually evaluated by not only geometric consistency but also color consistency. Since images in a mosaic data set may be captured by multisensors, at different illumination conditions or from different seasons, the color statistics inside a single image or between images are inconsistent, which will restrict their usages. The uneven illumination inside an image and the color differences between images are the two most important problems.

Uneven illumination removal is also called image dodging in remote sensing. Typically, remote-sensing image dodging methods contain homomorphic filtering, mask filtering, and

Manuscript received July 8, 2017; revised July 30, 2017; accepted August 19, 2017. Date of publication September 7, 2017; date of current version October 25, 2017. This work was supported in part by the National Natural Science Foundation of China under Grant 41271452 and Grant 41701528, in part by the Fundamental Research Funds for the Central Universities under Grant 2042017KF0235, and in part by the Key Technologies Research and Development Program of China under Grant 2015BAK03B04. (*Corresponding author: Jiayuan Li*.)

The authors are with the School of Remote Sensing and Information Engineering, Wuhan University, Wuhan 430079, China (e-mail: ljiy\_whu\_2012@whu.edu.cn; huqw@whu.edu.cn; aiminyao@whu.edu.cn).

Color versions of one or more of the figures in this letter are available online at <http://ieeexplore.ieee.org>.

Digital Object Identifier 10.1109/LGRS.2017.2743209

<sup>1</sup><https://sites.google.com/site/jiayuanli2016whu/home>

methods based on the retinex theory [1]. Homomorphic filtering [2] can separately process the illumination and reflectance of an image. According to frequency theory, the illumination distribution is related to the low frequency. Thus, homomorphic filtering applies a high-pass filter to remove uneven lightness. The main limitation is that the results may suffer from color distortion. Mask filtering [3] is based on an assumption that the uneven illumination phenomenon is caused by additional noise in an image. It then removes the background image based on the fast Fourier transform or wavelet transform. Obviously, this method may lose information; thus, color cast and partial blurring may appear in the results. Retinex theory [4] separates the lightness and color based on human visual perception. Jobson *et al.* [5], [6] presented single-scale retinex (SSR) for digital image enhancement; to alleviate halo artifacts, they extended SSR to multiscale retinex. Kimmel *et al.* [7] proposed a variational retinex (VR) technique to extract the illumination from an image based on energy function minimization. Li *et al.* [1] introduced a VR method for remote-sensing image dodging. However, the real hue of objects may be distorted by these retinex-based methods.

Color-correction methods can roughly be classified into two groups: parametric and nonparametric [8]. Parametric methods are also called model-based methods, and contain global and local methods. Global methods usually use a  $3 \times 3$  matrix to model the color relation between source and reference images. Gain compensation method [9] corrects intensity differences based on a diagonal model. It had been employed into a well-known commercial panoramic composition software called “Autopano” [10]. Mills and Gregory [11] adapted a linear approximation model for color tone correction. Tian *et al.* [12] estimated the global transformation by using a histogram mapping technique for images with overlapping regions. For images with no overlaps, Reinhard *et al.* [13] proposed a simple but effective method based on a linear model. They used statistics of color distributions to estimate the linear model. These methods cannot model complex color differences such as nonlinear differences. Li *et al.* [14] proposed a nonlinear photometric correlation method, which was called local moment matching (LMM). LMM considered regional tonal differences and used multiple pairs of gain and bias values to avoid overall luminance bias. Gamma correction model [15] is also a global model, which models more complex nonlinear color relations between images and has been widely used in camera imaging. Local modeling methods aim to build a finer mapping function. Tai *et al.* [16] proposed a probabilistic regional color-correction method based on the Gaussian mixture model and the expectation–maximization algorithm. However, local methods may suffer from boundary effect. Nonparametric methods usually correct images via histogram technique. For example, Yamamoto and Oi [17] used a joint histogram between two neighboring images for color correction.

1545-598X © 2017 IEEE. Personal use is permitted, but republication/redistribution requires IEEE permission.  
See [http://www.ieee.org/publications\\_standards/publications/rights/index.html](http://www.ieee.org/publications_standards/publications/rights/index.html) for more information.

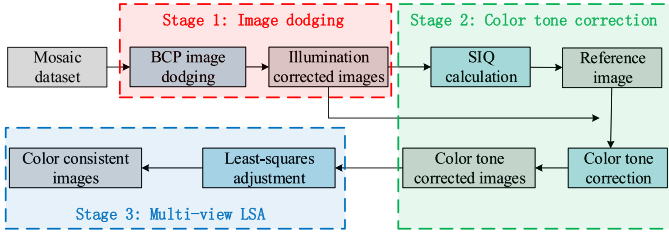


Fig. 1. Flowchart of the proposed optimal color consistency framework.

In this letter, we propose an optimal illumination and color consistency method. In this framework, we first present an image dodging algorithm based on bright channel prior (BCP) to remove the uneven illumination inside a single image. We also give a new single-image quality (SIQ) metric for automatic reference-image selection. Once the reference image is selected, a pairwise color-correction method based on a simplified gamma model is applied to coarsely align the color tone between source and reference images. Finally, we perform a least-square adjustment (LSA) procedure to obtain optimal illumination and color consistency among multiview images. Both synthetic and real experiments show that the proposed method outperforms the compared state-of-the-art approaches.

## II. OPTIMAL COLOR CONSISTENCY

The proposed color consistency method consists of three major stages, i.e., image dodging based on BCP, pairwise color correction, and multiview LSA. Fig. 1 gives the flowchart of the proposed method. As illustrated, we first perform BCP image dodging on a mosaic data set to remove uneven illumination distribution; then, we compute the SIQ value of each image to automatically select the reference image and correct the color tone of other images to be similar with the one of the reference image; finally, we perform an LSA procedure to obtain optimal color consistency among this mosaic data set.

### A. Image Dodging Based on BCP

In this section, we propose a single-image dodging algorithm based on BCP which is presented for shadow detection [18] task by us. According to the illumination–reflectance model, a scene image  $I$  is the product of illumination component  $L$  and reflectance component  $R$

$$I(x, y) = L(x, y)R(x, y) \quad (1)$$

where  $(x, y)$  is a pixel location in an image. For an image with uneven illumination distribution, our goal is to recover  $L$  from  $I$ . We introduce a simple but effective prior called BCP to simplify this underdetermined problem. The definition of BCP is that for a local patch inside an optical image, the reflectance of certain pixels is extremely high (close to 1) at least one channel

$$R^{\text{bcp}}(x, y) = \max_{c \in \{r, g, b\}} \left( \max_{(x', y') \in \Omega(x, y)} (R^c(x', y')) \right) \approx 1 \quad (2)$$

where  $R^{\text{bcp}}$  is the reflectance of BCP result;  $c \in \{r, g, b\}$  is a color channel in RGB color space; and  $\Omega(x, y)$  is the local patch of pixel  $(x, y)$ .

After performing twice max operation just like BCP formula on (1), we have

$$\begin{aligned} & \max_{c \in \{r, g, b\}} \left( \max_{(x', y') \in \Omega(x, y)} (I^c(x', y')) \right) \\ &= \max_{c \in \{r, g, b\}} \left( \max_{(x', y') \in \Omega(x, y)} (L(x', y')R^c(x', y')) \right). \end{aligned} \quad (3)$$

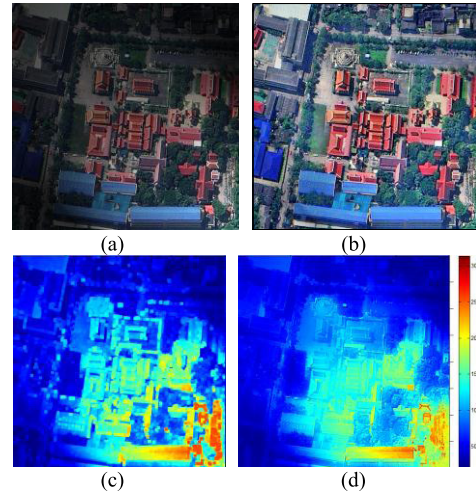


Fig. 2. (a) Cropped Worldview 2 image with uneven illumination. (b) Result after image dodging. (c) Illumination map obtained by (4). (d) Illumination map after guide filter refinement.

We assume that the illumination inside a small local patch  $\Omega(x, y)$  is continuous and tends to be a constant, denoted by  $\bar{L}_{\Omega(x, y)}$ . Thus, (3) can be rewritten as

$$\begin{aligned} & \max_{c \in \{r, g, b\}} \left( \max_{(x', y') \in \Omega(x, y)} (I^c(x', y')) \right) \\ &= \bar{L}_{\Omega(x, y)} \max_{c \in \{r, g, b\}} \left( \max_{(x', y') \in \Omega(x, y)} (R^c(x', y')) \right) \\ &= \bar{L}_{\Omega(x, y)} R^{\text{bcp}}(x, y) \approx \bar{L}_{\Omega(x, y)}. \end{aligned} \quad (4)$$

Since we assume that the illumination is a constant inside a local patch, illumination map obtained by (4) suffers from serious block effects [see Fig. 2(c)]. We then adopt fast guided filter to remove block effects and refine the illumination map [see Fig. 2(d)]. Finally, we remove the uneven illumination from the image and add an even lightness  $\hat{L}_{\Omega(x, y)}$  by

$$\hat{L}_{\Omega(x, y)} = (\bar{L}_{\Omega(x, y)})^\lambda \quad (5)$$

where  $\lambda > 1$ . Fig. 2(b) is the image dodging result of Fig. 2(a) by the proposed method. As can be seen, the final image has very impressed quality and the uneven illumination phenomenon has been removed.

### B. Pairwise Color Correction

Given a mosaic data set  $\{I_i\}_1^N$ , we first select an image from  $\{I_i\}_1^N$  with best quality as the reference image, denoted by  $I_{\text{ref}}$ , and then use a global model to represent the color relationship between other images and  $I_{\text{ref}}$ . Finally, other images are converted to have similar color tone with  $I_{\text{ref}}$ . Suppose that the uneven illumination phenomenon of this data set has been removed by the proposed image dodging algorithm. We use a simplified gamma correction model as the global model

$$I_{\text{ref}}^c = \left( \prod_{i \in \{r, g, b\}} I_i^c \right)^{\gamma^c} \quad (6)$$

where  $\gamma^c$  is a gamma coefficient of channel  $c \in \{r, g, b\}$ . Because the pairwise color-correction step is just an initial correction, whose role is to provide initial values for the following multiview LSA procedure, we use the mean intensity values of  $I_{\text{ref}}^c$  and  $I_i^c$  instead of pixel set intensity values to calculate  $\gamma^c$ :

$$m_{\text{ref}}^c = \left( \prod_{i \in \{r, g, b\}} m_i^c \right)^{\gamma^c} \quad (7)$$

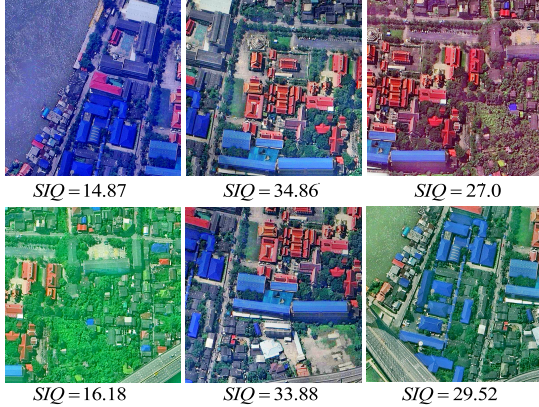


Fig. 3. SIQ value of each image in a Worldview 2 mosaic data set.

where  $m_{\text{ref}}^c$  and  $m_i^c$  are the mean intensity values of  $I_{\text{ref}}^c$  and  $I_i^c$ , respectively. Taking logarithm operation  $\text{In}(\cdot)$  on both sides of (7), the solution of  $\gamma^c$  can be obtained

$$\gamma^c = \text{In} \left( \frac{m_{\text{ref}}^c}{m_i^c} \right) / \text{In} \left( \frac{m_i^c}{m_{\text{ref}}^c} \right). \quad (8)$$

The key problem in this stage is the selection of reference image. We propose an SIQ metric that combines brightness deviation, color cast, and entropy together for automatic reference-image selection. As known, either too low overall brightness or too high overall brightness will decrease the quality of an image. Thus, we define the brightness deviation  $B_i^{\text{deviation}}$  as follows:

$$\begin{cases} \sigma_m = \sqrt{\frac{(3(m_i^r - 0.5))^2 + (6(m_i^g - 0.5))^2 + ((m_i^b - 0.5))^2}{46}} \\ B_i^{\text{deviation}} = (0.5 - \sigma_m)/0.5. \end{cases} \quad (9)$$

This function means that the images with overall brightness closer to middle intensity value (image intensity range is normalized to [0, 1]) have better quality. Color cast will also degrade the image quality. In other words, an image with better balance between different RGB channels has better quality. The formula to calculate color cast  $C_i^{\text{cast}}$  is given by

$$C_i^{\text{cast}} = 1 - \frac{\max_{c \in \{r,g,b\}} (m_i^c) - \min_{c \in \{r,g,b\}} (m_i^c)}{\max_{c \in \{r,g,b\}} (m_i^c)}. \quad (10)$$

Because image mosaicking data set usually covers the same object scene, the image with more detailed information is better. The proposed SIQ metric can be computed by

$$\text{SIQ}_i = B_i^{\text{deviation}} C_i^{\text{cast}} (E_i)^2 \quad (11)$$

where  $E_i$  is the entropy of an image  $I_i$ .

Fig. 3 shows the SIQ value of each image in a sample mosaic data set. As shown, the images in the middle column get the highest SIQ values, which are consistent with the human visual perception. Fig. 4 displays the pairwise color-correction results on this data set. The upper middle image is selected as the reference image according to SIQ values. As can be seen, these images almost have the same color tone with the reference image.

### C. Multiview LSA

As we only coarsely align the color tone between source and reference images, the color differences can still be observed.



Fig. 4. Pairwise color correction results on a Worldview 2 mosaic data set.



Fig. 5. Results of multiview LSA on Fig. 4.

For example, water region has a different color tone in the first image and last image of Fig. 4. To achieve an optical color consistency among a mosaic data set, we perform an LSA procedure to minimize the color alignment errors. Images inside a mosaic data set usually have overlapping regions with their nearby images. Thus, for an image pair  $I_i$  and  $I_j$  with an overlapping region, we use SIFT [19] algorithm and Lq-estimator [20] to extract reliable feature correspondences  $\{(x_k, y_k)\}_{k=1}^n$ , where  $\{x_k\}_{k=1}^n$  and  $\{y_k\}_{k=1}^n$  are image coordinates of feature points in image  $I_i$  and  $I_j$ , respectively. According to a global gamma correction model, we get

$$I_j^c(y_k) = (\alpha_{ij}^c I_i^c(x_k))^{\gamma_{ij}^c} \quad (12)$$

where  $I_i^c(x_k)$  is the pixel intensity of channel  $c$  of image  $I_i$  in location  $x_k$ ;  $\alpha_{ij}^c$  is a scale factor; and  $\gamma_{ij}^c$  is the gamma coefficient of the nonlinear gamma function. We first linearize the nonlinear function: performing logarithm operation on both sides of (12), we have

$$\text{In}(I_j^c(y_k)) = \gamma_{ij}^c (\text{In}(\alpha_{ij}^c) + \text{In}(I_i^c(x_k))). \quad (13)$$

Then, using the first-order Taylor expansion for (13)

$$\Delta f = f_{\gamma_{ij}^c} \Delta \gamma_{ij}^c + f_{\alpha_{ij}^c} \Delta \alpha_{ij}^c \quad (14)$$

where

$$\begin{cases} f(\gamma_{ij}^c, \alpha_{ij}^c) = \gamma_{ij}^c (\text{In}(\alpha_{ij}^c) + \text{In}(I_i^c(x_k))) \\ \Delta f = \text{In}(I_j^c(y_k)) - f(\gamma_{ij}^c, \alpha_{ij}^c) \\ f_{\gamma_{ij}^c} = \text{In}(\alpha_{ij}^c) + \text{In}(I_i^c(x_k)) \\ f_{\alpha_{ij}^c} = \gamma_{ij}^c / \alpha_{ij}^c. \end{cases} \quad (15)$$

Once we get a feature correspondence between any image pair inside the mosaic data set, we can add an equation to the LSA system. This system can be solved by the Gauss–Newton

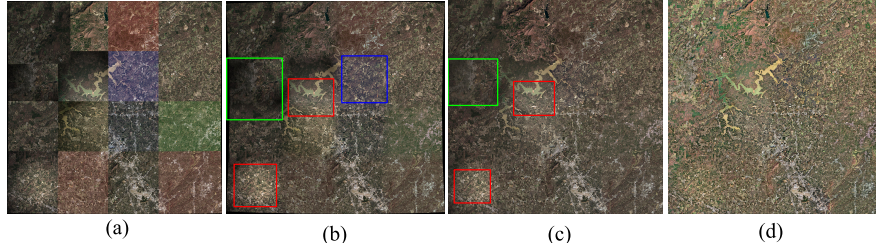


Fig. 6. Qualitative comparison on data set 1. The red box regions are too bright while the green box region is too dark in the results of Autopano and ICE, and the blue box region suffers from color cast phenomenon. (a) Result without correction. (b) Autopano result. (c) ICE result. (d) Our result.



Fig. 7. Qualitative comparison on data set 2. The green box regions are too dark and the blue box regions suffer from color cast phenomenon in the results of Autopano and ICE. (a) Result without correction. (b) Autopano result. (c) ICE result. (d) Our result.

method. Fig. 5 is the results after performing multiview LSA on the results displayed in Fig. 4. As can be seen, the color differences in the water region are much smaller than before.

### III. EXPERIMENTAL RESULTS

In this section, we report the performance comparisons between the proposed method and two other state-of-the-art methods, i.e., method used in Microsoft image composite editor software (ICE) [21] and method used in commercial software (Autopano) [10], on both synthetic and real remote-sensing data sets. There are two parameters in the proposed method, i.e., the size of local patch  $\Omega(x, y)$  and the even lightness factor  $\lambda$ . We set the size of  $\Omega(x, y)$  to 10 pixels and  $\lambda = 10$ . The parameters of Autopano, ICE, and our method are fixed throughout all the following experiments. All the experiments are performed on a laptop with i5, 2.5-GHz Intel Core.

#### A. Synthetic Data Comparison

Two synthetic mosaic data sets are used to evaluate the proposed method. The first synthetic data set (data set 1) comprised of  $4 \times 4$  images is cropped from a Landsat 8 OLI image with size  $3400 \times 3400$  pixels. The forward and side overlaps are 20%. The other one (data set 2) comprised of six images is cropped from a Worldview 2 image with size  $2000 \times 1500$  pixels. The forward and side overlaps are about 50%. The illumination and color of these cropped images are individually adjusted via Photoshop. Figs. 6(a) and 7(a) give simply mosaicked results without any color correction. As can be seen, the uneven illumination phenomenon and color differences are severe.

The qualitative comparisons of data set 1 are given in Fig. 6(b)–(d). As shown, the uneven illumination phenomenon and color tone differences are still observed in the result of Autopano. For example, the red box regions are much brighter than their adjacent regions while the green box region is much darker; the image pixels inside the blue box region are bluer than others. ICE gets very impressed color consistency. However, similar to Autopano, it also suffers from uneven illumination phenomenon. Our result is much better; that is, seamless color mosaicking is achieved. Fig. 7(b)–(d) gives the results of data set 2. Both Autopano and ICE suffer from illumination (green box region) and color tone (blue box

TABLE I  
QUANTITATIVE COMPARISONS

data	Entropy			SIQ		
	Autopano	ICE	ours	Autopano	ICE	ours
dataset 1	7.1	7.1	<b>7.6</b>	23.2	23.6	<b>36.2</b>
dataset 2	6.7	6.8	<b>7.4</b>	15.9	18.4	<b>36.5</b>
dataset 3	7.0	7.0	<b>7.6</b>	24.3	25.2	<b>42.9</b>
dataset 4	7.3	7.3	<b>7.6</b>	35.9	32.3	<b>45.7</b>

region) differences. Our method minimizes the color and illumination deviations. Table I reports the entropy and SIQ values of each method. ICE is slightly better than Autopano in both entropy and SIQ metrics, and our method gets the best.

#### B. Real Data Comparison

We also test the proposed method on two real remote-sensing mosaic data sets. The first real data set (data set 3) is comprised of eight aerial images with down-sampled size  $642 \times 1000$  pixels. The forward overlap is about 60%. The other one (data set 4) is comprised of four UAV images with down-sampled size  $800 \times 1000$  pixels. The forward overlap is about 30%. Figs. 8(a) and 9(a) give simply mosaicked results without any color correction. As shown, the illumination differences are severe.

The qualitative comparisons are given in Figs. 8 and 9. As shown, all the methods can achieve impressive results compared with simply mosaicked results. The borders inside Figs. 8(a) and 9(a) cannot be observed anymore after mosaicking; that is, the mosaicked results get color seamless. However, Autopano suffers from low overall brightness and low image contrast. ICE is sensitive to uneven illumination. For instance, the red box region in the ICE result of data set 4 is much brighter than the green one. Despite large color differences of input data sets, our method can brighten darker images, darken brighter regions, and correct color tone to be consistent with others. Each mosaicking result by the proposed method is just like a single good-quality image taken by a digital camera. Table I reports the entropy and SIQ values of each method. The proposed method gets much higher scores than both Autopano and ICE.

#### C. Running Time Analysis

Table II analyzes the time efficiency of the proposed method on an image pair selected from data set 1. (The size of each



Fig. 8. Qualitative comparison on data set 3. (a) Result without correction. (b) Autopano result. (c) ICE result. (d) Our result.

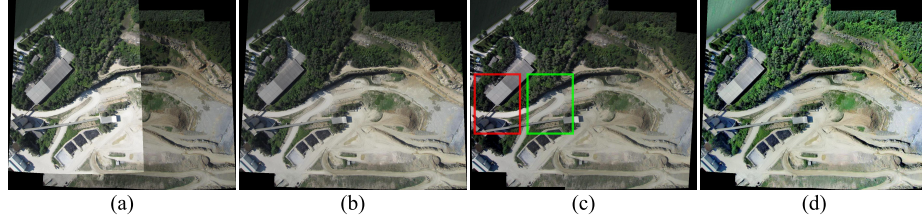


Fig. 9. Qualitative comparison on data set 4. The red box region is too bright while the green box region is too dark in the result of ICE. (a) Result without correction. (b) Autopano result. (c) ICE result. (d) Our result.

TABLE II  
RUNNING TIME ANALYSIS

Method stage	Running time/s
BCP image dodging	0.506
Pairwise color correction	0.384
Multi-view LSA	6.632
Model estimation	0.558

image is  $1000 \times 1000$  pixels.) As reported, the BCP image dodging and pairwise color tone correction stages are very fast; the multiview LSA stage is much slower than the first two stages. Multiview LSA spends more than 90% running time on SIFT feature matching. Fortunately, SIFT feature matching is usually performed in the image registration stage which obtains geometric consistency for image mosaicking. Thus, we can directly use the feature matching results of image registration stage. Thus, the total running time of the proposed method on these two images is about 1.45 s. In addition, if the source code of the proposed method is rewritten by C/C++, the time efficiency will be largely improved.

#### IV. CONCLUSION

In this letter, we proposed an effective technique for illumination and color seamless mosaicking. We first presented an image dodging algorithm based on BCP. We then used a simplified gamma correction model to coarsely align the color tone between the source and the reference images. We also proposed a simple but effective SIQ metric for automatic reference-image selection in this stage. To obtain optimal illumination and color consistency among input multiview images, we performed an LSA procedure to minimize the color differences. Extensive experiments on both challenging synthetic and real data sets show that the proposed method significantly outperforms the compared state-of-the-art approaches.

#### REFERENCES

- [1] H. Li, L. Zhang, and H. Shen, "A perceptually inspired variational method for the uneven intensity correction of remote sensing images," *IEEE Trans. Geosci. Remote Sens.*, vol. 50, no. 8, pp. 3053–3065, Aug. 2012.
- [2] M.-J. Seow and V. K. Asari, "Homomorphic processing system and ratio rule for color image enhancement," in *Proc. IEEE Int. Joint Conf. Neural Netw.*, vol. 4. Jul. 2004, pp. 2507–2511.
- [3] M. Wang and J. Pan, "A method of removing the uneven illumination for digital aerial image," *J. Image Graph.*, vol. 9, no. 6, pp. 744–748, 2004.
- [4] E. H. Land and J. J. McCann, "Lightness and Retinex theory," *J. Opt. Soc. Amer.*, vol. 61, no. 1, pp. 1–11, Jan. 1971.
- [5] D. J. Jobson, Z.-U. Rahman, and G. A. Woodell, "Properties and performance of a center/surround Retinex," *IEEE Trans. Image Process.*, vol. 6, no. 3, pp. 451–462, Mar. 1997.
- [6] D. J. Jobson, Z.-U. Rahman, and G. A. Woodell, "A multiscale Retinex for bridging the gap between color images and the human observation of scenes," *IEEE Trans. Image Process.*, vol. 6, no. 7, pp. 965–976, Jul. 1997.
- [7] R. Kimmel, M. Elad, D. Shaked, R. Keshet, and I. Sobel, "A variational framework for Retinex," *Int. J. Comput. Vis.*, vol. 52, no. 1, pp. 7–23, Apr. 2003.
- [8] W. Xu and M. Jane, "Performance evaluation of color correction approaches for automatic multi-view image and video stitching," in *Proc. IEEE Comput. Soc. Conf. Comput. Vis. Pattern Recognit. (CVPR)*, Jun. 2010, pp. 263–270.
- [9] Y. Du, J. Cihlar, J. Beaubien, and R. Latifovic, "Radiometric normalization, compositing, and quality control for satellite high resolution image mosaics over large areas," *IEEE Trans. Geosci. Remote Sens.*, vol. 39, no. 3, pp. 623–634, Mar. 2001.
- [10] M. Brown and D. G. Lowe, "Automatic panoramic image stitching using invariant features," *Int. J. Comput. Vis.*, vol. 74, no. 1, pp. 59–73, Aug. 2007.
- [11] A. Mills and D. Gregory, "Image stitching with dynamic elements," *Image Vis. Comput.*, vol. 27, no. 10, pp. 1593–1602, 2009.
- [12] G. Y. Tian, D. Gledhill, D. Taylor, and D. Clarke, "Colour correction for panoramic imaging," in *Proc. 6th Int. Conf. Inf. Vis.*, 2002, pp. 483–488.
- [13] E. Reinhard, M. Adhikmin, B. Gooch, and P. Shirley, "Color transfer between images," *IEEE Comput. Graph. Appl.*, vol. 21, no. 5, pp. 34–41, Sep./Oct. 2001.
- [14] X. Li, N. Hui, H. Shen, Y. Fu, and L. Zhang, "A robust mosaicking procedure for high spatial resolution remote sensing images," *ISPRS J. Photogramm. Remote Sens.*, vol. 109, pp. 108–125, Nov. 2015.
- [15] H. Farid, "Blind inverse gamma correction," *IEEE Trans. Image Process.*, vol. 10, no. 10, pp. 1428–1433, Oct. 2001.
- [16] Y.-W. Tai, J. Jia, and C.-K. Tang, "Local color transfer via probabilistic segmentation by expectation-maximization," in *Proc. IEEE Comput. Soc. Conf. Comput. Vis. Pattern Recognit. (CVPR)*, Jun. 2005, pp. 747–754.
- [17] K. Yamamoto and R. Oi, "Color correction for multi-view video using energy minimization of view networks," *Int. J. Auto. Comput.*, vol. 5, no. 3, pp. 234–245, 2008.
- [18] J. Li, Q. Hu, and M. Ai, "Joint model and observation cues for single-image shadow detection," *Remote Sens.*, vol. 8, no. 6, p. 484, 2016.
- [19] D. G. Lowe, "Distinctive image features from scale-invariant keypoints," *Int. J. Comput. Vis.*, vol. 60, no. 2, pp. 91–110, 2004.
- [20] J. Li, Q. Hu, and M. Ai, "Robust feature matching for remote sensing image registration based on  $L_q$ -estimator," *IEEE Geosci. Remote Sens. Lett.*, vol. 13, no. 12, pp. 1989–1993, Dec. 2016.
- [21] Microsoft. (Jun. 2017). *Image Composite Editor*. [Online]. Available: <https://www.microsoft.com/en-us/research/product/computational-photography-applications/image-composite-editor/>